Available online at www.sciencedirect.com

ScienceDirect

IFAC Papers Online
CONFERENCE PAPER ARCHIVE

IFAC-PapersOnLine 49-20 (2016) 214–219

Optimal Steady-State Temperature Field in an Experimental Annealing Furnace

L. Jadachowski * **A. Steinboeck** ** **A. Kugi** *

* *Christian Doppler Laboratory for Model-Based Control in the Steel Industry, Automation and Control Institute, Vienna University of Technology, Gußhausstraße 27-29, 1040 Vienna, Austria (e-mail: {jadachowski,kugi}@acin.tuwien.ac.at)*

** *Automation and Control Institute, Vienna University of Technology, Gußhausstraße 27-29, 1040 Vienna, Austria (e-mail: andreas.steinboeck@tuwien.ac.at)*

Abstract: The computation of an optimal steady-state operating point in an experimental annealing furnace is considered. In particular, the optimum spatial distribution of electric power supplied to IR-lamps is computed to ensure the temperature uniformity in the specimen fillet. A control-oriented reduced-order model of the steady-state 2D temperature distribution is derived and compared with the full-order model. Saturation functions are used to consider input constraints in a tailored optimization problem. The evaluation of the optimal control input is carried out with the full-order model. Uniqueness of the solution of the optimization problem is investigated numerically. The temperature field in the specimen fillet deviates less than 0.4 % of the setpoint value if sufficient heating power is available.

Keywords: Optimal operating point, Distributed-parameter systems, Elliptic quasilinear PDE, Model reduction, FE method, Non-equidistant grid

1. INTRODUCTION

Temperature uniformity control has a long tradition in manufacturing semiconductor devices, see, e.g., (Logerais et al., 2015; Ebert et al., 2004). In these applications, motivated by the manufacturing process of rotating circular wafers, the authors focus mostly on the temperature distribution along the radial coordinate by assuming uniform profiles along the tangential direction. Temperature uniformity along one spatial variable in vertical furnaces is also addressed by Shen et al. (2016).

While in continuous-type annealing furnaces (cf. Niederer et al., 2014) the temperature along the length of an axially moving strip is of main interest, in batch heating of flat specimens their 2-dimensional (2D) temperature profiles are in the focus of attention. This is especially true when dealing with a laboratory furnace as considered by Jadachowski et al. (2016) heated by electrically powered infrared (IR) radiators, where spatial non-uniformities of the specimen temperature may be caused by the usually fixed geometric arrangement of the IR-radiators and the specimen. The furnace under consideration is used by voestalpine Stahl GmbH to study and optimize process parameters of continuous annealing.

The heating chamber of the considered experimental annealing furnace is outlined in Fig. 1. It consists of a water-cooled housing with a steel specimen inside and two arrays of IR-lamps (N_h horizontal and N_v vertical IR-lamps) mounted on gold-coated water-cooled reflectors. The lamps are separated by the quartz glass windows from the annealing chamber filled with an inert atmosphere. Here, an inert gas streams into the heating zone through a gap between the upper specimen holder and the housing and leaves the IR-zone via the bottom gap. The quartz glass windows are fixed to the housing by means of gold-coated frames. When supplying electric power to the IR-lamps, the specimen of length L_s and width W_s is heated by means of thermal radiation. In particular, the temperature distribution in the specimen along the direction x is mainly influenced by the horizontal IR-lamps and the temperature distribution along the direction y is mainly determined by the vertical IR-lamps. The assumption of a homogeneous strip temperature along the direction z (direction of the specimen thickness B_s) is justified by the small Biot-number $Bi \ll 1$ (cf. Incropera et al., 2007). The temperature evolution in the specimen fillet $\Omega_f := \{(x,y) \in \mathbb{R}^2 \mid 0.25L_s < x < 0.75L_s,\ 0.2W_s < y < 0.8W_s\}$, with the area $A_f = L_f W_f$ and the dimensions $L_f = 0.5L_s$ and $W_f = 0.6W_s$, is subsequently of particular interest.

In this paper, an optimal steady-state operating point for a spatially 2D distributed-parameter model of the temperature evolution in a steel strip is determined. The goal is to optimize a steady-state distribution of electric power supplied to the IR-lamps to ensure the temperature uniformity in the specimen fillet during annealing. For this, an optimal control problem is formulated to minimize the mean temperature error between the specimen fillet and a desired reference temperature T_{ref}. In particular, a direct optimization (first discretize, then optimize) is applied based on a spatial discretization of the elliptic quasilinear partial differential equation (PDE) governing the stationary temperature profiles in the specimen. The

2405-8963
Peer review under responsibility of International Federation of Automatic Control.
10.1016/j.ifacol.2016.10.123

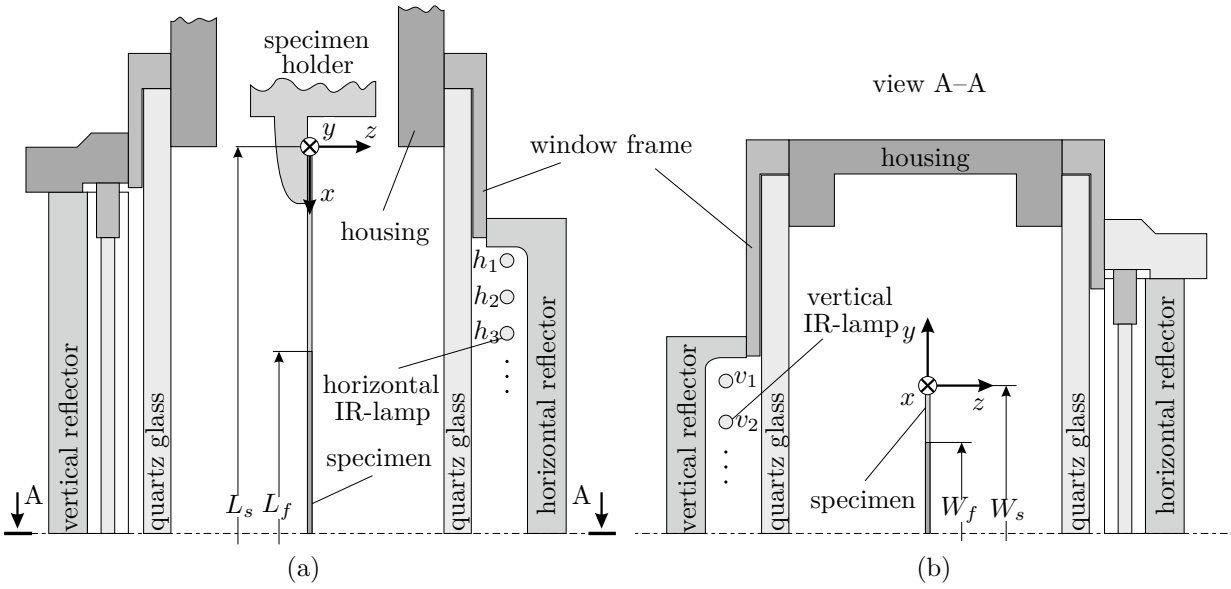

Fig. 1. Cross-sectional views of the experimental annealing furnace: (a) view from the side, (b) view from the top.

uniqueness of the solution of the considered optimization problem as well as the effect of the determined power distribution on the resulting temperature uniformity are investigated in numerical simulation studies.

The paper is structured as follows: In Section 2, the full-order finite difference model is summarized and a reduced finite element model is derived. In Section 3, an optimal steady-state control problem is formulated and saturation functions are used to incorporate input constraints. The latter is solved on the basis of the reduced model. Simulation results evaluated with the full-order model are presented and analyzed in Section 4. Final remarks given in Section 5 conclude the paper.

Notation: Arguments of functions are omitted whenever they are clear from the context. Moreover, $\nabla T(x,y,t) = [\partial_x T(x,y,t)\ \partial_y T(x,y,t)]$ denotes the temperature gradient with respect to spatial coordinates x and y with corresponding partial derivatives $\partial_x T(x,y,t)$ and $\partial_y T(x,y,t)$, respectively. Temperatures are assembled in the vector $\mathbf{T}_{(\cdot)} = \left[T_{(\cdot),i}\right]$. The vector of their fourth powers is written in the form $\mathbf{T}^4_{(\cdot)} = \left[T^4_{(\cdot),i}\right]$. Finally, $\mathbf{1}_n$ refers to the vector of dimension n with all entries equal to 1 and $\mathbf{I}$ is the identity matrix.

2. CONTROL-ORIENTED MODEL FOR SPECIMEN TEMPERATURE

The steady-state distribution of the specimen temperature along the spatial coordinates $(x,y) \in \Omega$ with $\Omega := \{(x,y) \in \mathbb{R}^2 \mid 0 < x < L_s,\ 0 < y < W_s\}$ is modeled by the non-local 2D quasilinear elliptic PDE

$$\operatorname{div}\big(\lambda(T)\nabla T(x,y)\big) + \dot{q}_r(x,y,T,\mathbf{u}) + \dot{q}_s(x,y,T) = 0 \quad (1)$$

with the 2D temperature profile $T(x,y)$ and the temperature-dependent thermal conductivity $\lambda(T)$. The control input $\mathbf{u}^{\mathrm{T}} = \left[\mathbf{u}_h^{\mathrm{T}}\ \mathbf{u}_v^{\mathrm{T}}\right]$ define the net radiative power emitted by the horizontal and vertical lamps with $\mathbf{u}_h = [u_{h,i}]_{i=1,\dots,N_h}$ and $\mathbf{u}_v = [u_{v,i}(t)]_{i=1,\dots,N_v}$. In fact, $u_{\star,i} = p^\star_{el,i}/(\pi d_\star l_\star)$ is the net heat flux at the surface of the lamp i with $\star \in \{h,v\}$, which has the effective diameter $d_\star$ and length $l_\star$. The electric power supplied to the lamp i is denoted by $p^\star_{el,i}$ and is assumed to be entirely converted into thermal radiative power. The source term $\dot{q}_r(x,y,T,\mathbf{u})$ depends explicitly on the input $\mathbf{u}$ and describes the thermal interaction between the specimen and surrounding surfaces. The heat source $\dot{q}_s(x,y,T)$ arises from to forced convection and heat conduction into the specimen holders.

The PDE (1) is completed by Robin type boundary conditions defined on $(x,y) \in \Gamma := \mathrm{cl}(\Omega) \setminus \Omega$, i.e.,

$$\lambda(T)\partial_x T(x,y) = \alpha_h\left(T(x,y) - T_h^{up}\right), \qquad x = 0 \quad (2a)$$
$$\lambda(T)\partial_x T(x,y) = -\alpha_h\left(T(x,y) - T_h^{lo}\right), \qquad x = L_s \quad (2b)$$
$$\lambda(T)\partial_y T(x,y) = \alpha_{ig}\left(T(x,y) - T_{ig}(x)\right), \qquad y = 0 \quad (2c)$$
$$\lambda(T)\partial_y T(x,y) = -\alpha_{ig}\left(T(x,y) - T_{ig}(x)\right), \qquad y = W_s \quad (2d)$$

with the convective heat transfer coefficients α_h, α_{ig}. The boundary disturbances $T_h^\dagger$, $\dagger \in \{up, lo\}$ and $T_{ig}(x)$ describe the temperature of the upper and lower specimen holder and the mean inert gas temperature along the specimen length, respectively.

2.1 Finite Difference Model of the Heat Conduction PDE

In view of the non-trivial character of (1) and (2), an early lumping approach is pursued. The domain Ω is spatially discretized into $N_s = N_x N_y$ equal rectangular elements $k = 1,\dots,N_s$ with side lengths $dx = L_s/N_x$ and $dy = W_s/N_y$. Based on the bijective mapping

$$(i,j) \mapsto k := i + N_x(j-1) \quad (3)$$

with $i = 1,\dots,N_x$ and $j = 1,\dots,N_y$, (1) and (2) are approximated using central difference quotients (Stoer and Bulirsch, 2002). This yields the finite difference (FD) approximation of (1) and (2) in the form

$$\mathbf{D}(\mathbf{T})\mathbf{T} + \dot{\mathbf{q}}_r(\mathbf{T},\mathbf{u}) + \dot{\mathbf{q}}_s(\mathbf{T}) + \mathbf{b}(\mathbf{T}) = 0 \quad (4)$$

with the state vector $\mathbf{T} = [T_k]_{k=1,\dots,N_s}$ and $T_k = T(x_i,y_j)$. In (4), $\mathbf{D}(\mathbf{T})$ describes heat diffusion in the specimen, $\dot{\mathbf{q}}_r(\mathbf{T},\mathbf{u})$ contains the net radiative heat fluxes between element surfaces and surrounding surfaces, convective and conductive heat sources are addressed by $\dot{\mathbf{q}}_s(\mathbf{T})$, and $\mathbf{b}(\mathbf{T})$ refers to the boundary conditions (2). Spatial discretizations $\dot{\mathbf{q}}_r(\mathbf{T},\mathbf{u})$ and $\dot{\mathbf{q}}_s(\mathbf{T})$ of the terms $\dot{q}_r(x,y,T,\mathbf{u})$ and $\dot{q}_s(x,y,T)$ can be found in (Jadachowski et al., 2016).